NJC

ROYAL SOCIETY OF CHEMISTRY

PAPER

View Article Online
View Journal | View Issue

Cite this: *New J. Chem.*, 2025, 49, 3930

Fluorescence detection of spermine and spermidine using a poly-carboxylate receptor and ensemble-based formalin sensing in real samples†

Sulekha Kumari Pandit and Gopal Das *

Received 18th November 2024,
Accepted 4th February 2025

DOI: 10.1039/d4nj04965a

rsc.li/njc

Spermine and spermidine, biogenic aliphatic polyamines, are essential clinical markers, but their extreme polarity and UV inactivity make their detection difficult. This study aims to develop a new receptor TP, which showed high selectivity for biogenic amines in fluorometric turn-on detection, with a response time of <5 seconds. The limit of detection was found to be 15.29 nM (3.07 ppb) and 10.29 nM (2.08 ppb) for spermine and spermidine, respectively. The interaction was primarily electrostatic, which led to disaggregation. Additionally, the host–amine ensemble was used for formalin detection. The potential for the real-world application of this receptor was demonstrated by fabricating a portable test kit, which not only exhibits its capability in detecting biogenic amines in an aqueous environment, but also in its qualitative estimation of the freshness of fish and chicken.

1. Introduction

Biogenic amines (BAs) are tiny chemical compounds that possess a high level of biological activity. They are often used as biomarkers in clinical settings to diagnose and monitor various diseases, including cancer, neurological disorders, and cardiovascular diseases.[1] They are primarily produced in the tissues of living organisms as a consequence of the decarboxylation of amino acids or the amination and transamination of aldehydes and ketones. These are primarily found in foods that are high in protein, such as animal products, like fish, poultry, mutton, and beef.[2] Nevertheless, since their concentration can rapidly increase upon deterioration, they might be considered to be quality indices. As soon as the food goes bad, the generation of BAs increases as a result of decarboxylation, which poses a possible threat to human health. BAs are found in fresh foods, but they are present in low concentrations.[3] In addition to this, amines have been utilized in our everyday lives as well as in industrial applications, such as in the production of refrigerants. In their natural state, the majority of amines are hazardous substances and even carcinogenic.[2]

As a result of the fact that these BAs are the products of microbial degradation of amino acids that are present in protein and that they are a possible signal for the rotting of specific foods, it is essential to identify them to guarantee the safety and quality of meat, fish, and dairy products. Spermine (SPM), spermidine (SPD), putrescine (PUT), histamine, dopamine, and other BAs are included among the most often discovered BAs. Two major polyamines, known as spermine (SPM) and spermidine (SDM), are among the various BAs. The essentiality of assaying spermine and spermidine in real samples stems from their relevance in medical diagnostics, where accurate measurement of their concentrations can provide valuable insights into a patient's health status.[4] These BAs have structures that are comparable to one another, and they can be utilized to evaluate the quality of meat products. The presence of SPM and SPD in the human body at levels that are higher than 0.5 nmol mL^{-1} (500 nM) has the potential to result in significant health issues, including but not limited to irregular blood pressure, headaches, and tachycardia or worsened asthma.[5,6] It is for this reason that the detection of SPM and SPD is of utmost significance and has the potential to contribute to the assurance of the safety of meat supplements.[7,8]

However, the detection of spermine and spermidine presents significant challenges due to their chemical properties. These compounds are highly polar and UV-inactive, making them difficult to detect using conventional techniques like UV-Vis spectroscopy.[9] Conventional analytical methods, such as gas chromatography-mass spectrometry (GC-MS), high-performance liquid chromatography (HPLC), and capillary electrophoresis (CE), often require extensive sample preparation, sophisticated instrumentation, and expertise, which can limit their practical application in real-world, on-site or point-of-care diagnostics. Furthermore, these methods tend to be time-consuming, costly and may require derivatization steps to enhance sensitivity, which adds complexity.[10]

Department of Chemistry, Indian Institute of Technology Guwahati, Assam 781039, India. E-mail: gdas@iitg.ac.in; Tel: +91 361 258 2313

† Electronic supplementary information (ESI) available: Characterization data, detailed spectral data, *etc*. See DOI: https://doi.org/10.1039/d4nj04965a

Recent advances in analytical chemistry have explored novel approaches like fluorescence-based detection, which offer greater sensitivity, selectivity, and ease of use, especially when paired with innovative receptor systems.[11] However, these newer methods must still have challenges related to interference from sample matrices and the need for highly sensitive, real-time detection systems suitable for practical use in clinical environments.

Therefore, a sensor that is not only easy to use but also portable and can effectively detect biogenic amines is very desirable for this application. In the pursuit of this objective, molecular fluorophore-based indicators have shown themselves to be a great player that is not only simple to manage but also a more cost-effective technique. In recent years, a variety of organic and inorganic[12–14] compounds and nanoparticles[15–17] have been utilized as optical receptors for the detection of spermine/spermidine.

On the same note, formaldehyde, which is also referred to as formalin (HCHO), is a volatile liquid at room temperature that mainly exists as a gas, is extremely hazardous, and colorless, and is also referred to as a killer gas when it is at room temperature.[18] Since it is emitted by products used in the home, it is one of the most significant polluting gases. It poses a threat to human health that is long-lasting. Exposure to formaldehyde over an extended period can have negative consequences on human health, including allergic reactions to the skin, mucosa, and respiratory system.[18–20] Formaldehyde is also suspected of being a potentially carcinogenic substance.[21] Conventional sensors that are utilized for formalin are heated metal oxide semiconductors; however, these sensors are not selective and exhibit cross-sensitivity to other gases.[22] Electrochemically based sensors are selective, although they have a lower sensitivity than other types of sensors. As a result, the development of a technology that is efficient, sensitive, and portable for the detection of formaldehyde is extremely desirable. As is common knowledge, aldehyde is capable of easily reacting with amine derivatives, resulting in the formation of matching imines through the Schiff base reaction. There is evidence in some of the more recent research that amines can be used for the detection of formalin sensing.[23–28] This property, along with the *in situ* production of a reaction between formalin and the amine in question, will result in the formation of a Schiff base, as well as the regeneration of the TP molecule, which will result in the fluorescence returning to its origin.

Therefore, as an extension of our ongoing research aimed at the advancement of fluorescent sensors,[29–38] we have reported a naphthalene-based receptor to detect spermine and spermidine in both the solution and vapor phases with a fluorescence turn-on response. In addition, the *in situ* reaction amine ensemble was utilized in the sensing of formalin, an indicator of the need for meat and fish to be discarded.

2. Results and discussion

2.1. Design principle of the receptors

For effective amine recognition, it is crucial to have a chemosensor with a slightly acidic nature that facilitates selective interaction with specific bases. This was accomplished by utilizing naphthalene as the fluorophoric unit and incorporating a tri-acidic unit that serves as both the interaction site and aids in increasing the molecule's polarity and solubility in water. Contrarily, another receptor was synthesized with aliphatic chains replacing the polar groups. This modification rendered the molecule hydrophobic and eliminated the interaction site. The purpose was to investigate if other parts of the molecule would exhibit any form of interaction. The TP and TPC receptors were successfully synthesized with a high yield (Scheme 1). As mentioned, the objective was to investigate the interaction of various biogenic amines.

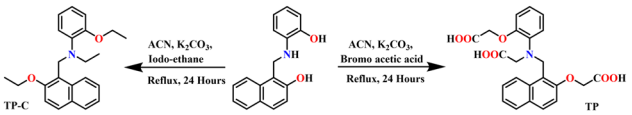

Scheme 1 Synthetic scheme of the receptors TP and TPC.

2.2. Photophysical studies of the receptors

The distinctive absorption peak of TP at 430 and 330 nm is attributed to the n–π and π–π* transitions (Fig. S11a, ESI†). Similarly, TPC exhibits two distinct absorption peaks observed at 400 and 330 nm. The absorbance of both receptors increased with the concentration (Fig. S11a, ESI†). The baseline of TPC has experienced a significant upliftment, indicating the formation of aggregates due to its hydrophobic core. Carboxylate group TP allows the molecule to dissolve in water (Fig. S11b Inset, ESI†) freely. The fluorescence spectra exhibited consistent findings across several concentrations, demonstrating a direct correlation between fluorescence intensity and concentration. At a lower concentration of 1 μM, the maximum intensity (I_{max}) was primarily observed at 418 nm. As the concentration was raised, the peak at 440 nm rose in intensity, eventually reaching the same level as the 418 nm peak and becoming the dominant emission peak (Fig. 1a). In the case of TPC around a lower concentration of 1 μM, the maximum intensity (I_{max}) was predominantly observed

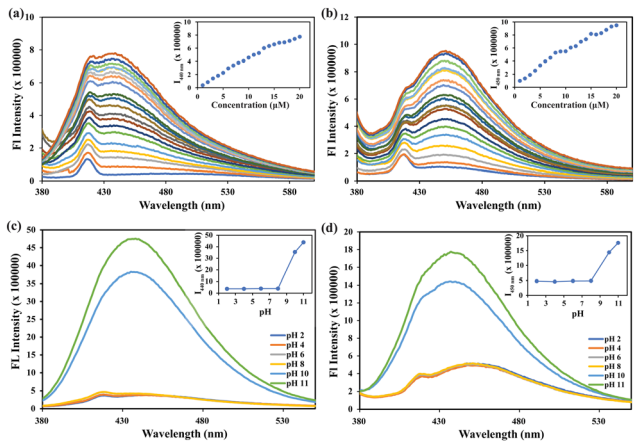

Fig. 1 (a) Fluorescence intensity *vs.* concentration of (a) TP and (b) TPC in water (Inset: Conc. *vs.* Fl intensity). Fluorescence intensity at different pH of (c) TP and (d) TPC (Inset: pH *vs.* Fl intensity).

around 418 nm and as the concentration is increased the peak at 450 nm becomes more prominent (Fig. 1b), finally becoming the dominant emission peak. This is accompanied by a steady shift towards longer wavelengths in the spectra, indicating the formation of better aggregates compared to TP. At higher concentrations, self-quenching should have been more noticeable; however, the fluorescence of both receptors remains nearly constant probably due to the development of aggregates. The activity of the substance at various pH levels was thoroughly examined to assess its utility in physiological conditions. No significant alterations were seen for both the receptors in UV-visible spectroscopy. However, the fluorescence intensity increases 12-fold from pH 2 to 12 (Fig. 1c) for TP, which is attributed to the deprotonation of the acid groups. However, the control compound TPC exhibited a 4-fold increase in fluorescence intensity at pH 12 (Fig. 1d). The fluorescence intensity exhibited minimal variation between pH 2–7 for both of the receptors. These data indicate that both receptors exhibit high sensitivity at alkaline pH levels. Therefore, their potential sensing towards basic molecules was investigated.

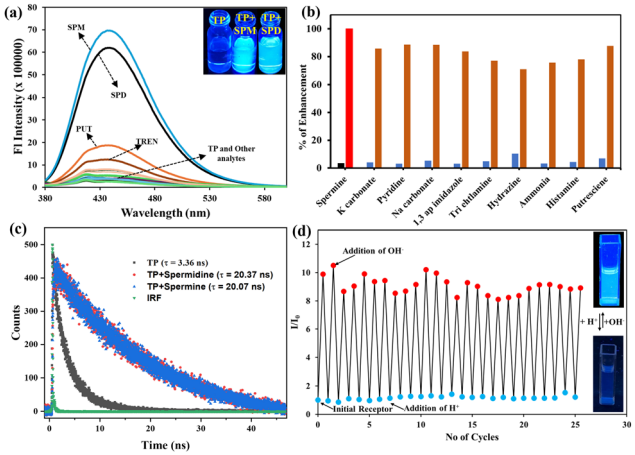

Fig. 2 (a) Fluorescence spectra of TP (10 μM) in the presence of different analytes (amines, cations, anions) in water. (b) Interference test of spermine in the presence of other biogenic amines and some bases (1(black) TP, (red) TP + SPM, Blue = TP + analytes, orange = TP + analytes + SPM). (c) Time-resolved photoluminescence (TRPL) data for TP and in the presence of spermine and spermidine using 375 lasers. (d) Reversibility of "ON–OFF" fluorescence intensity with the addition of acid and base.

2.3. Interaction of the receptor with biogenic amines

The presence of the carboxylate group and tertiary amine make the receptor (TP) a potential host for both metal ions, bases/amines, and anions, respectively. For this reason, the following ions/analytes were tested for any alteration in the spectroscopic property of the receptors: Al^{3+}, Mn^{2+}, Cr^{3+}, Fe^{3+}, Co^{2+}, Ni^{2+}, Pb^{2+}, Hg^{2+}, Cd^{2+}, Zn^{2+}, Cu^{2+}, Ag^{2+}, Ba^{2+}, Sn^{2+}, In^{3+}, Ti^{2+}, F^{-}, Cl^{-}, Br^{-}, I^{-}, NO_3^{-}, AcO^{-}, SO_4^{2-}, HSO_4^{-}, $H_2PO_4^{-}$, OH^{-}, PO_4^{3-}, SO_3^{-}, OCl^{-}, HIO_4, BO_3^{-}, ClO_4^{-}, CN^{-}, H_2O_2, $S_2O_3^{2-}$, K_2CO_3, pyridine, Na_2CO_3, triethylamine, hydrazine, ammonia, spermine (SPM), spermidine (SPD), putrescine (PUT), dopamine, histamine, TREN, 1,3-aminopropyl imidazole, EDTA. However, no changes were observed in UV-Vis spectroscopy (Fig. S13, ESI†) for a wide range of analytes, signifying that no noteworthy interactions are happening in the ground state of the receptor. Interestingly it was found that exclusively spermine and spermidine had a turn-on response in fluorescence spectroscopy (Fig. 2a). There was a small increment in fluorescence intensity in the case of putrescine due to the similarity in the structure with spermine (SPM) or spermidine (SPD). Other chemically similar analytes did not induce any significant change in the fluorescence emission of TP (Fig. 2a). Around a 21-fold increase for SPM and an 18-fold increase for SPD were detected. However, no changes were observed for TPC in the presence of these amines (Fig. S14, ESI†) in the aqueous environment.

The response of TP recorded was fairly quick enough and the results were obtained within 5 s of analyte addition. The exceptional selectivity towards spermine and spermidine compelled us to assess their capacity in the presence of different amines/bases. The results were consistent and similar enhancement were observed, and no interference was found with that of other amines/bases that could potentially act as interferants due to similar pK_a values (Fig. 2b). The interference was further conducted with similar inorganic species (Fig. S22 and S23, ESI†), which resulted in similar observations exhibiting high selectivity towards spermine and spermidine. A more thorough examination was conducted by gradually increasing the concentration of spermine/spermidine, resulting in a consistent and proportional increase in intensity from 4 to 20 μM (Fig. S15a, ESI†) where saturation was reached. To investigate this further, a graph was plotted between the concentration of spermine/spermidine and fluorescence emission intensity (Fig. S15 inset, ESI†). The experiment showed a linear relationship between the concentration and emission intensity, indicating that it is possible to accurately estimate the concentration of spermine/spermidine. The calibration curve gave a limit of detection of 15.29 nM (3.07 ppb) and 10.29 nM (2.08 ppb) for spermine and spermidine, respectively (Fig. S16a and S17b, ESI†), signifying TP to be superior to existing methods in terms of sensitivity and selectivity (Table S3, ESI†). The Benesi–Hildebrand equation was used to calculate the binding constant of the receptor and spermine/spermidine through the linear regime (Fig. S16b and S17b, ESI†). The value obtained was 3.9×10^4 M^{-1} and 6.6×10^4 M^{-1} for spermine and spermidine, respectively, indicating strong chelation and high sensitivity. A Job's plot was used to validate the binding stoichiometry by varying the mole fraction from 0 to 1 for TP and spermine/spermidine complexation, which showed the formation of a 1 : 1 complex (Fig. S16c and S17c, ESI†). This was further confirmed *via* mass spectrometry, which showed a 1 : 1 ratio for the mass peaks for the complex with ammonium ions (Fig. S18, ESI†). It was discovered that the fluorescence quantum yield was determined by using quinine sulfate as the standard (Table S1, ESI†). The analysis revealed that the addition of spermine/spermidine resulted in an increase in the quantum yield from 3.7% to 73 and 58% for spermine/spermidine, respectively. Fluorescence lifetime was measured for TP and TP with the spermine/spermidine. The decay was found to best fit in bi-exponential decay for TP of lifetime as 3.36 ns but on the addition of

spermine/spermidine, the lifetime increased to 20.07 and 20.37 ns with mono-exponential decay fit for the spermine and spermidine complex (Fig. 2c). The overall findings well correlate with the exceptional sensing toward spermine and spermidine.

2.4. Reversibility

The utilization of reusable fluorophores for the detection of BAs is not well-established in this field because these fluorophores mostly undergo reactions with BAs, making it challenging to restore them to their original condition. Upon recognizing the potential interpretation, we anticipated the receptor's reversible nature when exposed to acid. No alterations were noticed in the UV-visible spectroscopy in the presence of acid or base (Fig. S12, ESI†). There was a remarkable change in fluorescence spectroscopy on the addition of acid and base. The acid, namely hydrochloric acid (HCl), can break down the salt and disrupt other relationships, allowing it to revert to its original state for subsequent use. Hence, we conducted a reversibility experiment using NaOH as a model for BAs, as it shares similar features in terms of basicity. The receptor demonstrated reversibility for 26 cycles (Fig. 2d) while maintaining the initial fluorescence intensity. Simultaneously, the solution exhibited rapid switching of fluorescence, which was easily detectable under a UV 365 light. The fluorescence intensity remained consistent with no significant decrease noted. This demonstrates that the receptor has excellent pH reversibility and has the potential for repeated use. Therefore, this receptor may be used multiple times for practical purposes.

2.5. Formalin sensing with the host⊂amine ensemble

As we all know, aldehyde can easily combine with amine derivatives to make imines through the Schiff base reaction. Therefore, several reactive aldehydes, including formaldehyde, acetaldehyde, butyraldehyde, crotonaldehyde, and benzaldehyde, were detected by applying the selectivity of the host⊂amine sensing response. Fig. 3a shows that the emission intensity of the host amine was practically unaffected by the addition of aldehydes other than formaldehyde.

The quenching response of the host⊂amine towards the different analytes was estimated. Fig. 3c shows an 89% quenching efficiency (Fig. 3c) and Fig. S19c (ESI†) shows a 95% quenching efficiency for the spermine and spermidine complex, indicating a high selectivity to formaldehyde. Upon the addition of formaldehyde to the host⊂amine complex solution, which had a concentration ranging from 0 to 2 mM, there was a notable reduction in the emission intensity at 440 nm (Fig. 3b). Nevertheless, the emission intensity of the host⊂amine was nearly completely recovered upon the addition of 0.5 mM of formaldehyde in the instance of spermine (Fig. 3b inset). However, the initial fluorescence for spermidine was observed at a concentration of 2 mM (Fig. S19b, ESI†). A calibration graph was constructed to illustrate the linear relationship between the concentration of aldehyde and the response of the host⊂amine. The limit of detection (LOD) for the host⊂amine's sensitivity to HCHO was determined to be 630 μM (Fig. S20a, ESI†) and 1.45 mM (Fig. S20c, ESI†), based on the calibration graph.

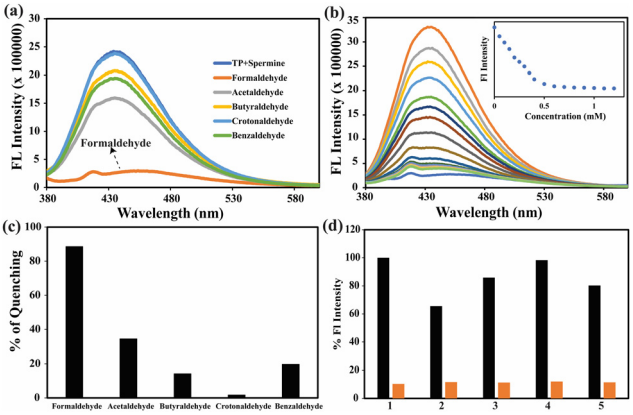

Fig. 3 (a) Sensing of formalin in the presence of other aldehydes with the TP⊂spermine ensemble; (b) fluorescence titration of HCHO to TP⊂spermine ensemble (Inset: Emission intensity at 440 nm as a function of the concentration of HCHO added); (c) bar graph representing the percentage of quenching in the presence of different aldehydes for the TP⊂spermine ensemble; (d) interference in the presence of a different aldehyde. {Black = TP⊂spermine + other aldehyde, orange = TP⊂spermine + other aldehyde + HCHO, 1 = formaldehyde, 2 = acetaldehyde, 3 = butyraldehyde, 4 = crotonaldehyde, 5 = benzaldehyde}.

The binding constant value for the complex formed between the host⊂amine with formaldehyde (HCHO) was determined using the Benesi–Hildebrand equation. The computed values were 3.5×10^4 M^{-1} (Fig. S20b, ESI†) for the complex with spermine and 4.2×10^4 M^{-1} (Fig. S20d, ESI†) for the complex with spermidine. This indicates that the host⊂amine exhibits a high level of sensitivity towards HCHO. To determine the selectivity towards different aldehydes, an interference test was conducted, and it was found that the host⊂amine ensemble was highly selective towards formalin (Fig. 3d) for the spermine ensemble and even in the presence of another similar aldehyde (Fig. S19d, ESI†). These findings confirm the efficiency of this receptor in differentiating and detecting formalin.

2.6. Plausible mechanism

To comprehend the change in fluorescence behavior, we have examined the interaction between the TP (electron donor) and the spermine/spermidine (electron acceptor). The receptor interacts with the analyte molecules spermine and spermidine, resulting in the formation of an acid–base adduct. This adduct formation occurs in a 1:1 ratio and causes the molecule to disaggregate, leading to a rise in fluorescence intensity. Furthermore, the development of a 1:1 adduct has been demonstrated by the HRMS (Fig. S18, ESI†) and Jobs's plot. There was a possibility of electrostatic interaction leading to charge transfer; this was further illustrated by zeta potential that shows that the overall charge in the receptor is −2.7 mV and the overall charge of SPM/SPD was 3.1 mV and 2.5 mV, respectively. When both of the solutions were mixed in water, the complex formed had overall charge near to 0 mV (SPM −0.7 mv, SPD −0.2 mV) making the overall complex neutral. The disaggregation has been corroborated by the morphological analysis and DLS analysis. The DLS analysis revealed that

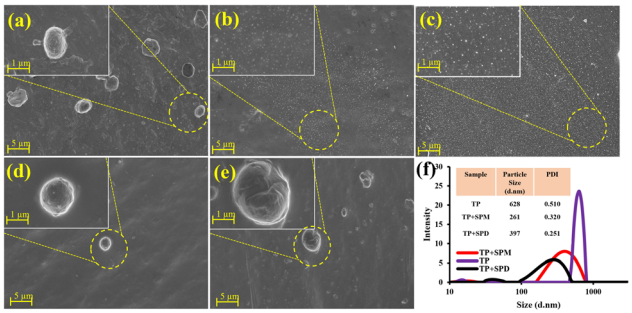

Fig. 4 FESEM images (a) TP, (b) TP + SPM, (c) TP + SPD, (d) TP⊂SPM + HCHO and (e) TP⊂SPD + HCHO. (f) Particle size analysis through DLS.

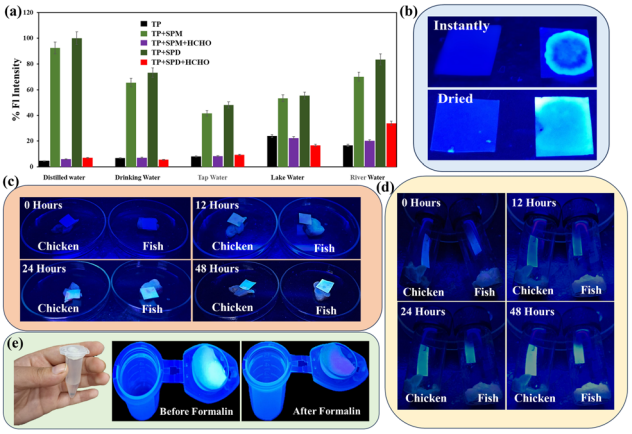

Fig. 5 (a) Changes in emission intensity of TP and TP⊂SPM/TP⊂SPD at 440 nm in different natural sources of water. (b) Photographs of the test strips under a UV lamp (irradiation of 365 nm) for visual detection of biogenic amines. (c) Biogenic amine sensing by TP and its utility as a food spoilage detector (images at room temp) under UV light before and after spoilage of chicken and fish when placed in direct contact. (d) Biogenic amine sensing by TP and its utility as a food spoilage detector under UV light before and after spoilage of chicken and fish when not placed in direct contact (vapor phase). (e) Formalin sensing in the vapor phase by the test strips of TP⊂SPM/TP⊂SPD.

the average particle size of 628 nm was reduced to 261 nm and 397 nm for the spermine and spermidine complex, respectively (Fig. 4f). FESEM analysis indicates the disintegration of spherical particles measuring 3.70 μm into microscopic particles measuring 272 nm and 176 nm during the creation of complexes involving spermine and spermidine (Fig. 4a–c). On interaction with aldehyde, the amine forms a Schiff-base imine product. The reaction of an aldehyde with the amine in the ensemble releases back the free receptor in the solution. This is supported by the reversing back of the original fluorescence intensity (Fig. 3a). Along with this, FESEM also supported a similar phenomenon wherein the original morphology was obtained as that of the receptor (Fig. 4d and e). Further computational studies were carried out using density functional theory (DFT) calculations with the B3LYP/6-31G method basis set and Gaussian 09 program, the optimized geometry shows the formation of more stable species (Fig. S21, ESI†). The optimized structure shows the change in dihedral angle from 149.5° to 140.6° symbolizing the structural changes that are happening due to deprotonation reducing the non-radiative decay process, which leads to enhancement in the fluorescence intensity.

2.7. Detecting biogenic amines in real samples

To assess the practicality of the receptor for real-life use, it underwent testing in different water systems and food samples. To accomplish this, a portable test kit was created and utilized to assess the efficacy of the receptor in detecting the presence of SPM/SPD in various water samples, including drinking water, tap water, lake water, and river water. Before spiking the water samples with a known concentration of SPM/SPD, solid contaminants were eliminated using filtration. Subsequently, emission spectra were promptly recorded. The recovery percentage was determined by calculating the proportion of detected substances in distilled water, assuming a 100% detection rate, using the spectral characteristics. As shown in Fig. 5a, the findings demonstrated the efficacy of the probes in a natural water system, with a retrieval rate of 72–79% for spermine and 74–83% for spermidine.

Formalin yielded significantly improved results when tested in various water samples, with a maximum recovery rate of 90%, even in the case of tap water (Table S2, ESI†). Fig. 5a demonstrates the effectiveness of the receptor in detecting substances in water samples obtained from natural sources.

To enhance the utilization of the receptor, it is possible to employ portable paper strips as a more practical and efficient approach for detecting SPM/SPD. The initial stage of this procedure entailed the application of TP onto Whatman filter paper (grade 1), which was thereafter left to dry naturally. Subsequently, the dried paper was submerged in a solution containing SPM/SPD. Upon inspection with a portable UV 365 nm lamp, the paper exhibited a distinct and intense blue fluorescence, as depicted in Fig. 5b. However, the hue of the paper remained unchanged when examined in visible light. The utilization of portable paper strips in combination with a smartphone sensing platform could offer a dependable method for visual and on-site detection.

The identical paper strips were employed to detect the level of freshness in chicken and fish. The poultry/seafood was purchased from a nearby market and meticulously washed with distilled water. The chicken/fish pieces were positioned on a sterile Petri plate, and the paper strip coated with TP was placed on top of them. It was noted that the paper strips were initially non-fluorescent, which indicated the freshness of the chicken or fish. Over time, the chicken/fish underwent degradation, resulting in the production of biogenic amines. As a result, the paper strip exhibited fluorescence. By the time 48 hours had passed, the meat had entirely deteriorated, causing the paper to become fully luminous (Fig. 5c). Similar results were obtained when the vapor phase of biogenic amines was tested, as shown in Fig. 5d. The paper strips were not brought into touch and were suspended nearby. As the vapors were released, the paper became bright. This suggests that the paper strips were equally effective in detecting biogenic amines in the form of vapor.

2.8. Application of the TP⊂amine ensemble

As previously mentioned, portable test kits were created utilizing Whatman filter paper. The ensemble exhibiting intense

blue fluorescence was employed for the detection of formalin vapors. The paper strip adhered to the top of a 5 mL Eppendorf tube, and formalin was added to the tube containing MeOH. The Eppendorf was securely sealed and gently heated to a temperature of 40 °C to facilitate the evaporation of dissolved formalin, while ensuring that methanol remains unaffected. According to the observation in Fig. 5e, the paper exhibited strong fluorescence before being exposed to formalin. However, after coming into contact with formalin, the paper strip lost its fluorescence. This demonstrates that the receptor ensemble can detect formalin not only in its liquid form but also in its gaseous form.

3. Conclusions

In conclusion, we have developed a turn-ON fluorogenic receptor (TP) that exhibits significant selectivity for SPM/SPD in aqueous environments. The receptor demonstrated remarkable selectivity and sensitivity for SPM/SPD amidst different competing metal cations, anions, and amines, including other analogous biogenic amines. A remarkably low limit of detection was attained, which is much lower than detecting any potential risk as early as possible has been effectively utilized for assessing the freshness of meat and fish when adapted to portable paper strip formats. Comparison of receptors with other fluorescent probes indicates that TP exhibits superior performance, particularly in terms of LOD values and anti-interference capability. The TP-SPM and TP-SPD ensembles were subsequently employed to detect formalin demonstrating their wide application potential. We have confidence that this receptor will significantly contribute to the investigation of biological functions.

4. Experimental section

4.1. Materials and methods

All reagents and solvents were obtained from commercial sources and used as received without further purification. Solvents for synthesis and further experiments were purchased from Merck, India, and used as received. ^{1}H NMR spectra were recorded on a 400 MHz instrument and ^{13}C NMR was recorded on a 600 MHz instrument, and chemical shifts were recorded in parts per million (ppm) on the scale using tetramethylsilane [$Si(CH_3)_4$] or a residual solvent peak as a reference. The mass spectra (ESI-MS) of the receptors were recorded in methanol. IR spectra of both the receptors were recorded on a PerkinElmer FT-IR spectrometer as KBr disks in the range 4000–450 cm^{-1}. A UV-Vis spectrophotometer and Horiba Fluoromax-4 spectrofluorometer were used for UV-visible and fluorescence experiments. Recording of the UV-vis spectra was done in 10 mm path-length quartz cuvettes in the range of 300–600 nm wavelength, while fluorescence measurement was done using a 10 mm path-length quartz cuvette with a slit width of 5 nm at 25 °C.

4.2. Synthesis and characterisation

4.2.1. Receptor SR. This was synthesized *via* the reported literature.[39] 2-Hydroxy naphthaldehyde and 2-amino phenol were reacted in a 1 : 1 ratio in MeOH under reflux for 12 hours. A bright orange precipitate was obtained, and it was cooled to RT. In ice-cold conditions, a pinch of $NaBH_4$ was added until the solution turned colorless, the solution was further kept under reflux for 12 hours. The resultant solution was then concentrated and diluted with an equal volume of water to obtain a brick-colored precipitate. This was characterized *via* HRMS (Fig. S1, ESI†) and used without purification. ESI-MS (positive mode, *m*/*z*): mass spectrum of TP, calculated for $C_{17}H_{15}NO_2$ = 265.1103, obtained $[M + H]^+$ = 266.1176.

4.2.2. Receptor TP. 1-(((2-Hydroxyphenyl)amino) methyl)-naphthalene-2-ol (0.2 gm, 0.753 mmol) was dissolved in acetonitrile (ACN). To this solution, K_2CO_3 was added (0.416 gm, 3.01 mmol) and kept on stirring for about 30 min; then bromoacetic acid (0.627 gm, 4.51 mmol) was added to the mixture and kept under reflux for about 24 hours. The reaction mixture was monitored *via* TLC. DCM–water workup was done with 5% aqueous HCl. The organic layer was concentrated and the product obtained was chocolate brown colored and was highly hygroscopic and hence stored in a desiccator (60% yield).

^{1}H NMR (400 MHz, DMSO-d_6) δ (ppm): δ 7.85 (d, J = 8.0 Hz, 1H), 7.76 (d, J = 8.0 Hz, 1H), 7.61 (d, J = 8.0 Hz, 2 H), 7.44 (t, J = 8.0 Hz, 2H), 7.27 (t, J = 8.0 Hz, 2H), 7.16 (d, J = 8.0 Hz, 2H), 2.41 (s, 2H), 1.24 (s, 6H) (Fig. S2, ESI†). ^{13}C NMR (151 MHz, DMSO-d_6) δ 166.99, 152.17, 138.95, 134.18, 128.89, 128.54, 127.96, 126.44, 125.93, 124.23, 123.22, 122.62, 119.87, 119.18, 118.54, 20.89, 14.54, 10.88 (Fig. S3, ESI†). ESI-MS (positive mode, *m*/*z*): mass spectrum of TP, calculated for $C_{23}H_{21}NO_8$ = 439.1267, found $[TP + H]^+$ = 440.1340 (Fig. S4, ESI†). FT-IR (ν, cm^{-1}): 3058(O–H stretching), 2924 (C–H alkyl), 1654 (C═O), 1095 (C–O stretching) (Fig. S5, ESI†).

4.2.3. Receptor TPC. 1-(((2-Hydroxyphenyl)amino) methyl)-naphthalene-2-ol (0.2 gm, 0.753 mmol) was dissolved in ACN. To this solution, K_2CO_3 was added (0.416 gm, 3.01 mmol) and kept on stirring for about 30 min; then, iodo-ethane (0.703 gm (375 μL), 4.51 mmol) was added to the mixture and kept under reflux for about 24 hours. The reaction mixture was monitored *via* TLC. DCM–water workup was done with 5% aqueous HCl. The organic layer was concentrated and the product obtained was chocolate brown coloured and was highly hygroscopic and hence stored in a desiccator (70% yield).

^{1}H NMR (400 MHz, DMSO-d_6) δ (ppm): δ 8.13 (d, J = 8.0 Hz, 1H), 7.94 (d, J = 8.0 Hz, 1H), 7.85 (d, J = 8.0 Hz, 1H), 7.79 (d, J = 8.0 Hz, 1H), 7.58 (t, J = 8.0 Hz, 1H), 7.47 (t, J = 8.0 Hz, 2H), 7.39 (t, J = 8.0 Hz, 2H), 7.27 (d, J = 8.0 Hz 1H), 4.37 (t, J = 8.0 Hz, 2H), 4.17 (q, J = 8.0 Hz, 2H), 2.53 (s, 2H), 1.36 (q, J = 8.0 Hz, 3H), 1.23 (t, J = 8.0 Hz, 6H), 0.869 (s, 2H) (Fig. S6, ESI†). ^{13}C NMR (151 MHz, DMSO-d_6) δ 153.83, 153.74, 138.61, 129.08, 128.68, 128.68, 128.35, 127.59, 126.63, 124.33, 123.33, 123.71, 123.67, 118.95, 115.41, 64.98, 30.88, 29.49, 15.54, 14.41, 10.98 (Fig. S7, ESI†). ESI-MS (positive mode, *m*/*z*): mass spectrum of TPC, calculated for $C_{23}H_{27}NO_2$ = 349.2042, found $[TPC + H]^+$ = 350.2115 (Fig. S8, ESI†). FT-IR (ν, cm^{-1}): 2926 (C–H alkyl stretching), 1240 (C–O stretching) (Fig. S9, ESI†).

Author contributions

Sulekha Kumari Pandit: design, conception, data acquisition/analysis, data interpretation as well as drafting of the manuscript. Gopal Das: writing and reviewing, editing, supervision, and funding acquisition.

Data availability

The datasets supporting this article have been uploaded as part of the ESI.†

Conflicts of interest

There are no conflicts to declare.

Acknowledgements

We thank and acknowledge DBT (BT/NER/143/SP44675/2023) and DST (SR/FST/CS-II/2017/23C), New Delhi, India, for their financial support. We also recognize the instrumental facilities provided by the Central Instrument Facility (CIF) and the Department of Chemistry at IIT Guwahati. SKP acknowledges IIT Guwahati for the fellowship and help of Mr Sayan Samanta for the initial synthesis of the compounds.

References

1 M. Czerwiński, A. Bednarska-Czerwińska, N. Zmarzły, D. Boroń, M. Oplawski and B. O. Grabarek, *J. Clin. Med.*, 2021, **10**, 4872.
2 S. Koutros, C. F. Lynch, X. Ma, W. J. Lee, J. A. Hoppin, C. H. Christensen, G. Andreotti, L. B. Freeman, J. A. Rusiecki and L. Hou, *Int. J. Cancer*, 2009, **124**, 1206–1212.
3 A. Önal, *Food Chem.*, 2007, **103**, 1475–1486.
4 A. W. Maksymiuk, D. S. Sitar, R. Ahmed, B. Cheng, H. Bach, R. A. Bagchi, N. Aroutiounova, P. S. Tappia and B. Ramjiawan, *Future Sci. OA*, 2018, **4**, FSO345.
5 L. F. Cohen, D. W. LUndgren and P. M. Farrell, *Blood*, 1976, **48**(3), 469–475.
6 B. Del Rio, B. Redruello, D. M. Linares, V. Ladero, P. Ruas-Madiedo, M. Fernandez, M. C. Martin and M. A. Alvarez, *Food Chem.*, 2018, **269**, 321–326.
7 S. Chopra, A. Singh, P. Venugopalan, N. Singh and N. Kaur, *ACS Sustainable Chem. Eng.*, 2017, **5**, 1287–1296.
8 M. Papageorgiou, D. Lambropoulou, C. Morrison, E. Kłodzińska, J. Namieśnik and J. Płotka-Wasylka, *TrAC, Trends Anal. Chem.*, 2018, **98**, 128–142.
9 A. Boffi, G. Favero, R. Federico, A. Macone, R. Antiochia, C. Tortolini, G. Sanzó and F. Mazzei, *Anal. Bioanal. Chem.*, 2015, **407**, 1131–1137.
10 M. A. Munir and K. H. Badri, *J. Anal. Methods Chem.*, 2020, 5814389.
11 X. Fang, Y. Zheng, Y. Duan, Y. Liu and W. Zhong, *Anal. Chem.*, 2018, **91**, 482–504.
12 R. R. Nair, S. Debnath, S. Das, P. Wakchaure, B. Ganguly and P. B. Chatterjee, *ACS Appl. Bio Mater.*, 2019, **2**, 2374–2387.
13 R. Tejpal, M. Kumar and V. Bhalla, *Sens. Actuators, B*, 2018, **258**, 841–849.
14 M. Barros, S. Ceballos, P. Arroyo, J. A. Sáez, M. Parra, S. Gil, A. M. Costero and P. Gaviña, *Chemosensors*, 2021, **10**, 8.
15 K. W. Wong, T. H. Tsoi and C. W. Kan, Direct Colorimetric Detection of Spermine using Gold Nanoparticles, WO2020224571A1, 2020.
16 X. Tan, X. Liu, W. Zeng, Z. Zhang, T. Huang, L. Yu and G. Zhao, *Spectrochim. Acta, Part A*, 2019, **221**, 117176.
17 S. Chopra, A. Singh, P. Venugopalan, N. Singh and N. Kaur, *ACS Sustainable Chem. Eng.*, 2017, **5**, 1287–1296.
18 D. B. Go, M. Z. Atashbar, Z. Ramshani and H.-C. Chang, *Anal. Methods*, 2017, **9**, 4112–4134.
19 S. Das, S. Kumar, J. Singh and M. Kumar, *Sens. Actuators, B*, 2022, **367**, 132114.
20 S. Das, A. Kumar, J. Singh and M. Kumar, *Sens. Actuators, B*, 2023, **387**, 133824.
21 J. H. Arts, M. A. Rennen and C. de Heer, *Regul. Toxicol. Pharmacol.*, 2006, **44**, 144–160.
22 N. Joshi, T. Hayasaka, Y. Liu, H. Liu, O. N. Oliveira and L. Lin, *Mikrochim. Acta*, 2018, **185**, 1–16.
23 N. Ding, Z. Li, Y. Hao and X. Yang, *Food Chem.*, 2022, **384**, 132426.
24 A. Bi, T. Gao, X. Cao, J. Dong, M. Liu, N. Ding, W. Liao and W. Zeng, *Sens. Actuators, B*, 2018, **255**, 3292–3297.
25 C. Liu, C. Shi, H. Li, W. Du, Z. Li, L. Wei and M. Yu, *Sens. Actuators, B*, 2015, **219**, 185–191.
26 J. Chen, K. Chen, B. Han, Y. Xue, W. Chen, Z. Gao and X. Hou, *Tetrahedron*, 2020, **76**, 131681.
27 B. Dong, X. Song, Y. Tang and W. Lin, *Sens. Actuators, B*, 2016, **222**, 325–330.
28 W. Zhou, H. Dong, H. Yan, C. Shi, M. Yu, L. Wei and Z. Li, *Sens. Actuators, B*, 2015, **209**, 664–669.
29 M. Basak and G. Das, *Analyst*, 2021, **146**, 6239–6244.
30 M. Basak and G. Das, *Spectrochim. Acta, Part A*, 2022, **280**, 121521.
31 O. A. Pegu, A. Das and G. Das, *J. Mol. Struct.*, 2023, **1294**, 136427.
32 S. K. Pandit, S. Das and G. Das, *Sens. Diagn.*, 2024, 136131.
33 R. Moral, O. A. Pegu and G. Das, *Dyes Pigm.*, 2023, **218**, 111502.
34 S. Halder, B. Nayak, B. Bhattacharjee, A. Ramesh and G. Das, *J. Mater. Chem. C*, 2021, **9**, 8596–8605.
35 S. Halder, B. Nayak, B. Bhattacharjee, A. Ramesh and G. Das, *J. Mater. Chem. C*, 2021, **9**, 8596–8605.
36 S. Samanta, C. Kar and G. Das, *Anal. Chem.*, 2015, **87**, 9002–9008.
37 C. Kar, B. Ojha and G. Das, *Luminescence*, 2013, **28**, 339–344.
38 S. K. Pandit and G. Das, *Sens. Actuators, B*, 2024, 136131.
39 J. H. Billman and A. C. Diesing, *J. Org. Chem.*, 1957, **22**, 1068–1070.

